Modelling of wall currents excited by plasma wall-touching kink and vertical modes during a tokamak disruption, with application to ITER

C.V. Atanasiu[1], L.E. Zakharov[2],K. Lackner[3], M. Hoelzl[3], F.J. Artola[4], E. Strumberger[3], X. Li[5]

[1]Institute of Atomic Physics, Bucharest, Romania (*atanasiu@ipp.mpg.de*)
[2]LiWFusion, Princeton, US
[3]Max Planck Institute for Plasma Physics, Garching b. M., Germany
[4]Aix Marseille Université, Marseille, France
[5]Academy of Mathematics and Systems Science, Beijing, P.R. China

17th European Fusion Theory Conference, Athens - Greece

October 9-12, 2017

Overview

1. Introduction & assumptions

• the nonlinear evolution of MHD instabilities - the **Wall Touching Kink Modes** (WTKM) - leads to a dramatic quench of the plasma current within *ms* $\longrightarrow$ very energetic electrons are created (runaway electrons) and finally a global loss of confinement happens $\equiv$ a **major disruption**;

• in the ITER tokamak, the occurrence of a limited number of major disruptions will definitively damage the chamber with no possibility to restore the device;

• the WTKM are frequently excited during the **Vertical Displacement Event** (VDE) and cause big sideways forces on the vacuum vessel [1, 2].

• **objective**: to consider in JOREK, STARWALL, JOREK-STARWALL the current exchange plasma-wall-plasma

Theoretical example: modelling of an axisymmetric vertical instability [Zakharov et. al, PoP (2012).]

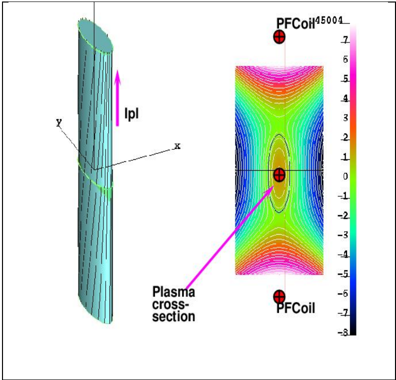

Theoretically simplest example of vertically unstable plasma:

1.Quadrupole field of externalPFCoils
2.Straigh tplasma column with uniform current along z-axis
3.Elliptical cross-section
4.Plasma is shifted downward from equilibrium
5.Plasma current is attracted by the nearest PF-Coil with the same current direction ≡ instability

Question: Where the plasma will go to?
The answer isn't trivial!

<table>
<tr>
<td>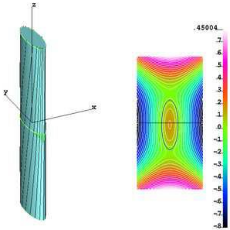
</td>
<td>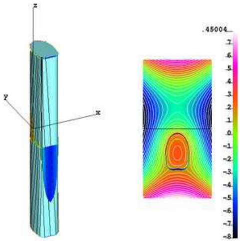
</td>
<td>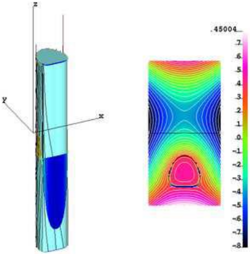
</td>
</tr>
<tr>
<td>Initial downward plasma displacement</td>
<td>Nonlinear phase of instability. Negative surface current at the leading plasma side</td>
<td>1.Strong negative sheet current at the leading plasma edge
2.Plasma cross-section becomes triangle-like</td>
</tr>
<tr>
<td colspan="3">(a) opposite poloidal field $B_\theta^{vac} \simeq -B_\theta^{core}$ across the leading plasma edge;
(b) two Null Y-points of poloidal field in the triangle-like plasma cross-section. Plasma should be leaked through the Y-point until full disappearance.
Strong external field stops vertical motion.</td>
</tr>
</table>

1) **Free boundary MHD modes**, which are always associated with the surface currents, are evident in the tokamak disruptions:
(a) excitation of m/n=1/1 kink mode during VDE on JET (1996),
(b) recent measurements of Hiro currents on EAST (2012).
2) Both theory and JET, EAST experimental measurements indicate that **the galvanic contact of the plasma with the wall is critical in disruption**;
3) **The thin wall approximation** is reasonable for thin stainless steel structures of the vacuum vessel (# 1-3 cm & $\sigma = 1.38 \cdot 10^{-6} \Omega^{-1} \mathrm{m}^{-1}$.)
4) For simulating the plasma-wall interaction during disruption, **the reproduction of 3D structure of the wall is important** (e.g., the galvanic contact is sensitive to the local geometry of the wall in the wetting zone [3].
5) Our **wall model** covers both **eddy currents**, excited inductively, and **source/sink currents** due to current sharing between plasma and wall.
6) We adopted a **FE triangle representation** of the plasma facing wall surface (- **simplicity** & - **analytical formulas for B** of a uniform current in a single triangle) [4].

2. Two kinds of surface currents in the thin wall

- **Helmholtz decomposition theorem** states that any sufficiently smooth, rapidly decaying vector field **F**, twice continuously differentiable in 3D, can be resolved into the $\sum$ of an irrotational (curl-free) vector field and a solenoidal (divergence-free) vector field;
- thus, the **surface current density** $h\mathbf{j}$ in the conducting shell can be split into **two components**: [3]

$$h\mathbf{j} = \mathbf{i} - \bar{\sigma}\nabla\phi^S \; ,$$
$$\mathbf{i} \equiv \nabla I \times \mathbf{n}, \quad (\nabla \cdot \mathbf{i}) = 0, \quad \bar{\sigma} \equiv h\sigma, \tag{1}$$

(a) $\mathbf{i}$ = the divergence free surface current (eddy currents) and
(b) $-\bar{\sigma}\nabla\phi^S$ = the source/sink current (S/SC) with potentially finite $\nabla\cdot$ in order to describe the current sharing between plasma and wall,
$\bar{\sigma} = h\sigma$ = surface wall conductivity, h =thickness of the current distrib.,
I = the stream function of the divergence free component (eddy currents),
$\mathbf{n}$ = unit normal vector to the wall,
ϕ^S = the source/sink potential ($\equiv$ surface function).

- The S/S-current in Eq. (1) is determined from the **continuity equation** of the S/S currents across the wall

$$\nabla \cdot (h\mathbf{j}) = -\nabla \cdot (\bar{\sigma}\nabla\phi^S) = j_\perp, \qquad (2)$$

- $j_\perp \equiv -(\mathbf{j} \cdot \mathbf{n})$ = the density of the current coming from/to the plasma, $j_\perp > 0$ for $j_\perp$ plasma $\longrightarrow$ wall.
- Faraday law gives

$$-\frac{\partial \mathbf{A}}{\partial t} - \nabla\phi^E = \bar{\eta}(\nabla I \times \mathbf{n}) - \nabla\phi^S, \quad \bar{\eta} \equiv \frac{1}{\bar{\sigma}} \qquad (3)$$

A=vec. pot. of **B**, ϕ^E= electric potential, $\bar{\eta}$=effective resistivity.

- Eqs. (2, 3) describe the current distribution in the thin wall, given the sources $j_\perp, B_\perp^{pl}, B_\perp^{coil}$ as $f(\vec{x}, t)$;
- Eq. (2) for ϕ^S is independent from Eq. (3), but contributes via $\partial B_\perp^S/\partial t$ to the r.h.s. of Eq. (3).

- for our numerical wall model, **A** can be calculated with:

$$\mathbf{A}^{wall}(\mathbf{r}) = \mathbf{A}^{I}(\mathbf{r}) + \mathbf{A}^{S}(\mathbf{r}) = \sum_{i=0}^{N_T-1} (h\mathbf{j})_i \int \frac{d\mathbf{S}_i}{|\mathbf{r} - \mathbf{r}_i|}, \tag{4}$$

with $\sum$ over the N_T FE triangles and the $\int$ is taken over Δ surface **analytically**.

- **the equation for the stream function** I is given by [4, 5]

$$\nabla \cdot (\frac{1}{\bar{\sigma}} \nabla I) = \frac{\partial B_\perp}{\partial t} = \frac{\partial (B_\perp^{pl} + B_\perp^{coil} + B_\perp^{I} + B_\perp^{S})}{\partial t} \tag{5}$$

$B_\perp^{pl,coil,I,S}$ = the perpendicular to the wall B component.

- **Biot-Savart relation** for B is necessary to close the system of Eqs..

3. Energy principle for the thin wall currents

- ϕ^S can be obtained by minimizing the **functional** W^S [3].

$$W^S = \int \left\{ \underbrace{\frac{\bar{\sigma}(\nabla\phi^S)^2}{2} - j_\perp \phi^S}_{minim.\ gives\ Eq.(2)} \right\} dS - \oint \underbrace{\phi^S \bar{\sigma}[(\mathbf{n} \times \nabla\phi^S)}_{S.C.\ \perp to\ the\ edges} \cdot d\vec{\ell}]. \qquad (6)$$

- $\int dS$ is taken along the wall surface,
- $\oint d\vec{\ell}$ is taken along the edges of the conducting surfaces with the integrand representing the surface current normal to the edges,
- $\oint d\vec{\ell}$ takes into account the external voltage applied to the edges of the wall and $=0$, as happens in typical cases.

- I can be obtained by minimizing the **functional** W^I [3]

$$W^I \equiv \frac{1}{2}\int\Bigg\{ \underbrace{\frac{\partial(\mathbf{i}\cdot\mathbf{A}^I)}{\partial t}}_{\textit{inductive term due to } \mathbf{i}} + \underbrace{\frac{1}{\bar{\sigma}}|\nabla I|^2}_{\textit{resistive loses}} + \underbrace{2\left(\mathbf{i}\cdot\frac{\partial \mathbf{A}^{ext}}{\partial t}\right)}_{\textit{excitation by other sources}} \Bigg\} dS - \underbrace{\oint(\phi^E-\phi^S)\frac{\partial I}{\partial \ell}d\ell}_{S.C.\ \perp\ \textit{to edges}} . \qquad (7)$$

4. Matrix circuit equations for triangle wall representation

- **the two energy functionals** for ϕ^S and for I are suitable for implementation into numerical codes and constitute **the electromagnetic wall model for the wall touching kink and vertical modes**;

- the substitution of I, ϕ^S as a set of plane functions inside triangles leads to **the finite element representation of W^I, W^S as quadratic forms for unknowns I, ϕ^S in each vertex**;

- the unknowns vectors at the N_V vertexes are

$$\vec{I} \equiv I_0, I_1, ..., I_{N_V-1}, \tag{8}$$
$$\vec{\phi}^S \equiv \phi_0^S, \phi_1^S, ..., \phi_{N_V-1}^S.$$

- the minimization of quadratic forms W^S and W^I

$$\partial W^S/\partial\vec{\phi}^S = 0,\ \ \partial W^I/\partial\vec{I}^n = 0,\ \partial W^I/\partial\vec{\phi}^S = 0,$$

leads to **linear systems of equations with Hermitian symmetric-positive definite matrices which can be solved using the Cholesky decomposition**: $\mathbf{W} = \underbrace{\mathbf{L}}_{\textit{lower triangular}} \bullet \underbrace{\mathbf{L}^*}_{\textit{conjugate transpose of } \mathbf{L}}$

- the matrix equations are [6]

$$\begin{aligned}
&\mathbf{W}^{SS}\cdot\vec{\phi}^S = -\vec{j}_\perp \\
&\mathbf{M}^{II}\cdot\frac{\vec{I}^n - \vec{I}^{n-1}}{\Delta t} + \mathbf{R}\cdot(\vec{I}^n - \vec{I}^{n-1}) + \mathbf{R}\cdot\vec{I}^{n-1} + \mathbf{W}^{IS}\cdot\frac{\vec{\phi}^{S,n} - \vec{\phi}^{S,n-1}}{\Delta t} \\
&= -\mathbf{A}^{IV}\cdot\frac{\partial(\vec{A}^{pl} + \vec{A}^{ext})}{\partial t},
\end{aligned} \tag{9}$$

with **vector sources** $\vec{j}_\perp \equiv \{j_{\perp,0},\ j_{\perp,1},\ j_{\perp,2},\ \ldots j_{\perp,N_V-1}\}$ and $\vec{A}^{pl,ext} \equiv \{\vec{A}_0^{pl,ext},\ \vec{A}_1^{pl,ext},\ \vec{A}_2^{pl,ext},\ \ldots\vec{A}_{N_V-1}^{pl,ext}\}$, with Δt = the "wall-time-step", superscript n = time slice.

- inverting the matrices $\mathbf{W}^{SS}$ and $\mathbf{M}^{II}$ the calculation of the wall currents is reduced to 2 relations implemented in our code

$$\begin{aligned}
\vec{\phi}^{S} &= -\left(\mathbf{W}^{SS}\right)^{-1} \cdot \underbrace{\vec{j}_{\perp}}_{input} \\
\vec{I}^{n} &= \underbrace{\vec{I}^{n-1}}_{input} - \widehat{\mathbf{R}} \cdot \underbrace{\vec{I}^{n-1}\Delta t}_{input} + \widehat{\mathbf{W}}^{IS} \cdot \underbrace{\frac{\partial \vec{j}_{\perp}}{\partial t}\Delta t}_{input} \\
&- \mathbf{A}^{IV} \cdot \underbrace{\frac{\partial(\vec{A}^{pl} + \vec{A}^{ext})}{\partial t}\Delta t}_{input}. \qquad (10)
\end{aligned}$$

- as **output**, the code returns the values of ϕ_i^S and I_i in all vertexes, allowing the calculation of the **A** and **B** of the wall currents in any point $\vec{r}$

5.1. Numerical solution [6, 7]

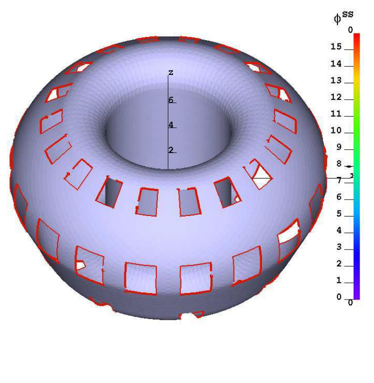

Fig.2 Identifying the FE edge elements in ITER wall

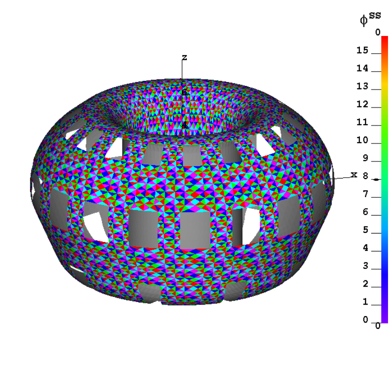

Fig.3 21744 FE triangle distribution in ITER wall

iVertex	σ*1e-6	h [m]	x [m]	y [m]	z [m]
0	1.380	0.0300	4.855455	-1.767241	-5.134041
1	1.380	0.0300	4.701757	-1.711300	-5.127522
2	1.380	0.0300	4.388355	-1.597231	-5.064147
3	1.380	0.0300	4.104409	-1.493883	-4.934104
4	1.380	0.0300	3.840408	-1.397794	-4.739096
5	1.380	0.0300	3.618104	-1.316882	-4.481675
...	....	.....	.....	.....	.....
11218	1.380	0.0300	4.935902	-1.994234	-5.127791
11219	1.380	0.0300	3.690935	-3.376420	-5.128447
11220	1.380	0.0300	3.758745	-3.525608	-5.134041
11221	1.380	0.0300	3.966048	-3.048552	-5.128447
11222	1.380	0.0300	4.124746	-3.089426	-5.134041

Table 1. *Vertexes, thickness h and σ distributions for the ITER wall.*

iTriangle	i[A]	i[B]	i[C]	Prop
0	641	0	1	0
1	641	1	58	0
2	641	58	57	0
3	641	57	0	0
.....	.....	.....	.....	.....
21741	11221	10350	11222	0
21742	11222	10350	10349	0
21743	11222	10349	10415	0

Table 2. *Triangles and correspondent vertexes distribution for the ITER wall.*

Matrix	Memory size [KB]
$(\mathbf{W}^{SS})^{-1}$	984,030
$\widehat{\mathbf{R}}$	855,106
$\widehat{\mathbf{W}}^{SS}$	917,305
$\widehat{\mathbf{A}}^{IV}$	917,305
$(\widehat{\mathbf{M}}^{II}_{\bar{\sigma}})^{-1}$	855,106

Table 3. *Matrices size for the 21744 triangles and 11223 vertexes of the FE discretization of ITER wall.*

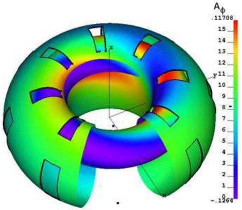

Fig. 4 Wetting zone created by a VDE and a kink m/n=1/1. The color of the wall =distribution of the perturbed *Aφ.*

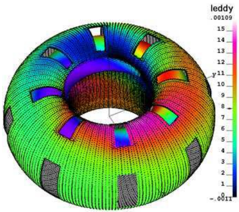

Fig. 5 Eddy currents excited by the plasma perturbation. The color corresponds to *I* stream function.

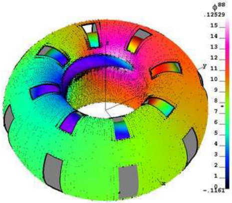

Fig. 6 Eddy currents excited by both plasma perturbation and S/S current. Distribution of Φ^S at the wall surface.

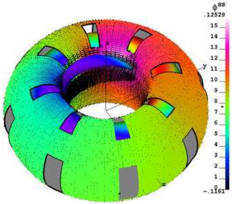

Fig. 7 Total surface current with the S/S current as the dominant component.

6.2. Analytical solution

- for a shell with elliptical cross-section and three holes (Fig. 8.1 with the correspondent geometry in a curvilinear coordinate system (u, v) in Fig. 8.2). For $h\sigma{=}1$, we have to solve the eq.

$$\nabla^2 \phi^S = j_\perp(u, v) \quad u = \text{toroidal coord.}, \quad v = \text{poloidal coord.},$$

with **pure homogeneous Neumann B.C.** and the following **existence condition** to be satisfied:

$$\int_\Omega j_\perp d\Omega = \int_{\partial\Omega} \nabla \phi^S \cdot \mathbf{n} dS$$

$$\Omega = \underbrace{\Omega_e}_{\textit{wall domain}} \setminus \underbrace{\Omega_i}_{\textit{hole domain}} \qquad \partial\Omega = \underbrace{\Gamma_e}_{\textit{wall boundary}} \sqcup \underbrace{\Gamma_i}_{\textit{hole boundary}} .$$

The analytical $\phi(u, v)$ has been chosen in the form [3, 5, 7]

$$\phi^S(u, v) = \int G_u(u) du \cdot \int G_v(v) dv, \quad \text{with}$$

$$G_u(u) = \Pi(u - u_{ik}); \quad G_v(v) = \Pi(v - v_{ik}); \quad i = 0, ..., 3, \; k = 1, 2,$$

If for 1 hole the relative error was of 0.003 for a grid with a mesh $32 \times 32 \times 4$, for 3 holes the error is ≈ 5 times greater.

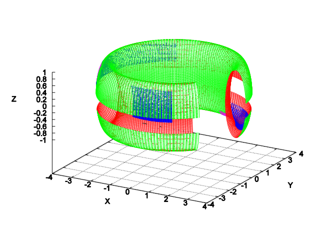

Fig. 8.1 Tokamak wall with elliptical cross-section and three holes (in blue).

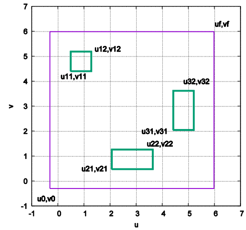

Fig. 8.2 Multiply connected test domain D(u,v) between the four rectangles in a curvilinear coordinate system (u,v)

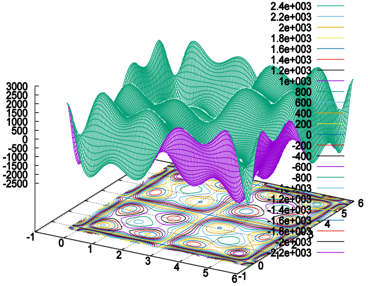

Fig. 8.3 Distribution of the analytical $\Phi^S(u,v)$ function.

6. Next steps

- to realize the connection with JOREK in order to obtain the following **input data**:

$$\vec{A}^{pl} + \vec{A}^{ext} = f(t, \mathbf{r})$$
$$\vec{J}_{\perp} = f(t, \mathbf{r})$$
$$\Delta t$$

- using this approach, JOREK-STARWALL [Merkel, Strumberger, arXiv:1508.04911 (2015), Hoelzl, Merkel et al., Journal of Physics: Conference Series (2012).] , presently limited to eddy currents, will be extended to self-consistent non-linear MHD simulations including eddy and source/sink currents.

- to include non-symmetrical wall structures

- to determine the iron core influence (like in JET) on surface currents [Atanasiu, Zakharov et al, Comp. Phys. Comm. (1992).]

7. Summary

- a rigorous formulation of the surface current eqs. was formulated;

- in the triangular representation of the wall surface, both surface current components are represented by the same model of a uniform current density inside each Δ;

- the coupling of finite element matrix equations for both types of currents contains the same matrix elements of mutual capacitance C_{ij} of two triangles $\Delta_{i,j}$ which can be calculated analytically;

- our model has been checked successfully on an analytical case;

- our code received the status of "open source license".

8. References

[1] L. E. Zakharov, Physics of Plasmas **15**, 062507 (2008).
[2] L. E. Zakharov, S.A. Galkin, S.N. Gerasimov, Physics of Plasmas **19**, 055703 (2012).
[3] L. E. Zakharov, C. V. Atanasiu, K. Lackner, M. Hoelzl, and E. Strumberger, J. Plasma Phys. **81**, (2015).
[4] C. V. Atanasiu and L. E. Zakharov, Phys. Plasmas **20**, 092506 (2013).
[5] C.V. Atanasiu, L.E. Zakharov, D. Dumitru, Romanian Reports in Physics **67**, 2, 564-572 (2015).
[6] L.E. Zakharov, C.V. Atanasiu,X. Li, *Interface of wall current modeling with disruption simulation codes*, JOREK-STARWALL discussion meeting, IPP, Garching bei München, Germany, March 10, 2017.
[7] C.V. Atanasiu, L.E. Zakharov, K. Lackner, M. Hoelzl, and E. Strumberger, *Wall currents excited by plasma wall-touching kink and vertical modes*, $3^{\rm rd}$ JOREK General Meeting, Prague, 20-24 March 2017.
[8] P Merkel, E Strumberger, arXiv:1508.04911 (2015).
[9] M. Hoelzl, P. Merkel, G.T.A. Huysmans, et al., Journal of Physics: Conference Series **401**, 012010 (2012).
[10] C.V. Atanasiu, L.E. Zakharov, and A. Moraru, Comp. Phys. Comm. **70**, 483-494 (1992).